Remote Sensing and Hydrology 2000 (Proceedings of a symposium held at Santa Fe, New Mexico, USA, April 2000). IAHS Publ. no. 267, 2001.

The impact of the structure and composition of shrub-coppice dune landscapes on MASTER reflectance anisotropy

M. CHOPPING, T. SCHMUGGE, A. RANGO, J. RITCHIE, W. KUSTAS

USDA-ARS Hydrology Laboratory, BARC-W, Beltsville, Maryland 20705, USA.
e-mail: chopping@hydrolab.arsusda.gov

JOHN R. VANDE CASTLE

Biology Department, University of New Mexico, Albuquerque, New Mexico 87131, USA

Abstract This study assesses the effects of physical structure and composition of shrub-coppice dune landscapes on anisotropy in the NASA MODIS-ASTER Airborne Simulator (MASTER) solar channels, and investigates the viability of simulating multi-angular data sets using off-nadir airborne imaging radiometry from a single overpass by means of data segmentation. Segmentation data are plant density and cover and spectral measures derived from high-resolution aerial photography and classified Landsat 7 Enhanced Thematic Mapper imagery. The directional signal contributes a variation of 5–10% in reflectance, necessitating angular corrections. For most areas the signal appears to differ only slightly with changes in landscape structure and composition because the view/illumination geometry is poor and reflectance is dominated by bright soils. Further work is required to determine whether simple models would be adequate for angular corrections.

Key words anisotropy; dunes; landscape; mesquite; multiple view angle; New Mexico; structure

INTRODUCTION

The primary mission of NASA's MASTER is to collect ASTER-like and MODIS-like land datasets to support the validation of the ASTER (Advanced Spaceborne Thermal Emission and Reflection Radiometer) and MODIS (MODerate-resolution Imaging Spectroradiometer) geophysical retrieval algorithms. A significant challenge to the use of MASTER data in MODIS and ASTER calibration and validation campaigns over land is presented by the large total field-of-view of 86°. Furthermore, the solar-target geometry is not necessarily the same for each mission. Because the land surface is not a Lambertian scatterer of downwelling radiation in the solar wavelengths (Kimes, 1983), optical remote sensing data depend importantly on the bidirectional reflectance distribution function (BRDF), which depends on the three-dimensional structure and optical properties of the materials in a sensor's instantaneous field-of-view (IFOV) and on canopy heterogeneity (Barnsley, 1994). Over semiarid environments, surface structure and canopy heterogeneity cause a large angular variation in spectral reflectance (Chopping, 2000). Not only is cover lower, but also soils are brighter and canopies more clumped than in temperate and humid regions. The sunlit and shaded proportions of the materials in a sensor's IFOV change with viewing angle and relative

azimuth, reducing the utility of unidirectional spectral data. Correction of off-nadir airborne data has been attempted via empirical adjustment of values to a preferred geometry by interpolation and extrapolation (Kennedy *et al.*, 1997) or band ratio techniques (Qi *et al.*, 1995), and by modelling the BRDF (Leroy & Bréon, 1996). Correction efforts are hampered by the fact that airborne scanners often make only one overpass of any area, limiting the range of geometries for each target. A suggestion for overcoming this is image segmentation by cover type in order to simulate a multi-directional dataset (Qi *et al.*, 1997). The quality of the directional signal retrieved will depend partly on the method used to segment the image data. Moreover, surface reflectance retrieval must account for atmospheric scattering and absorption.

OBJECTIVES

The main objective is to determine the magnitude and characteristics of the directional reflectance signal of mesquite shrub-coppice dune landscapes through its impact on MASTER reflectance data. A secondary objective is to investigate the viability of simulating multi-angular data sets using off-nadir airborne imaging radiometry from a single overpass by segmentation of the MASTER imagery.

METHODS

Test area

The test area is in the USDA-ARS Jornada Experimental Range, New Mexico (USA), the subject of numerous ecological and remote sensing experiments (Rango *et al.*, 1998; Privette & Asner, 1999). A key surface characteristic of these rangelands is the spatial heterogeneity and lacunarity of vegetation and soil patches (DeSoyza *et al.*, 1998). The study area is dominated by shrub-coppice dunes with honey mesquite (*P. glandulosa*) growing on them.

Surface spectral reflectance from MASTER data

The MASTER scene used was acquired on 27 September 1999 and calibration was performed at the Airborne Sensor Facility at NASA Ames Research Center. The ground-projected field-of-view (GIFOV) is ≈3.5 m at nadir. This MASTER dataset is of high quality since the atmosphere was very clear and dry with little contamination from clouds, sand or dust. Aerosol optical thickness was estimated at only 0.02–0.04 at 550 nm using sun photometer measurements made at the AERONET station at the Sevilleta National Wildlife Refuge (Holben *et al.*, 1998), 300 km to the north. Atmospheric profiles of temperature, water vapour and pressure were obtained from rawinsonde data from the nearby White Sands C-station radiosonde launch at 11:00 h GMT and normalized spectral response functions were interpolated from filter functions provided by Ames. The geometry of the MASTER acquisitions varies mostly

in the viewing plane and the solar-target geometry does not change much, allowing the calculation of a single series of 716 sets of transformation coefficients for surface reflectance retrieval using the 6S code (Vermote *et al.*, 1997), version 4.2. The MASTER GIFOV is small in relation to mesquite shrub diameters which are often >10 m (Rango *et al.*, 2000) so a single sample from the MASTER will not capture the directional signal of a cover type. Simulation of larger FOV data was therefore effected by convolution of the image with the point spread function (PSF) of a larger FOV sensor (MSS). The convolution kernel was a 27 × 27 matrix derived from the 7 × 7 MSS PSF given by Hlavka (1986). The resulting images were resampled to the grid spacing of a MSS North American Land Cover Triplicate image from 1992 (Fig. 1).

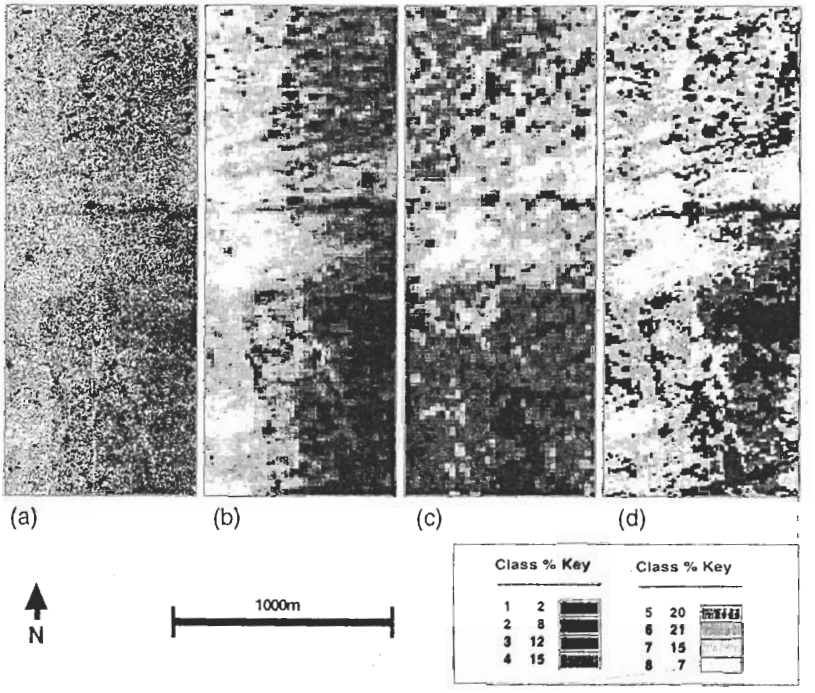

Fig. 1 Simulation of large GIFOV data and segmentation of study area: (a) MASTER channel 5 (0.666 μm) reflectance at ~3.5 m; (b) convolved with typical 27 × 27 Point Spread Function on 60 m grid; (c) Landsat MSS channel 2 reference image (5 August 1992) at 60 m; (d) ISODATA classification of Landsat ETM+ solar channel DNs (28 September 1999).

Segmentation data

The BRDF is dependent on canopy heterogeneity and lacunarity as well as optical properties; it is therefore useful to identify locations which are similar in plant density and cover. Structural information for segmentation was derived from aerial photography and classified Landsat 7 Enhanced Thematic Mapper (ETM+) imagery. Large format aerial photography, digitized to a 5504 row by 4756 column high-resolution image (≈0.33 m^2), was used to calculate shrub count and standard

deviation and total vegetation cover for a moving 90 × 90 window (30-cell interval). Vegetation objects were additionally defined by minimum and maximum cell counts; density and area statistics were obtained for small (snakeweed and yucca) and large (honey mesquite) plant types. The size criteria were obtained through reference to ground photographs linked to dune and vegetation maps made using LIDAR and multispectral aerial videography (Rango *et al.*, 2000). The NIH Image Particle Analysis algorithm performs well in isolating vegetation from the soil background even where the local contrast between these is very low (Fig. 2). Cover and shrub density images (not shown) for all shrubs are not highly correlated, indicating that each contains different information on the landscape. The study area was segmented into eight classes using the Iterative Self-Organizing Data Analysis Technique (ISODATA) algorithm. A subscene from a Landsat 7 ETM+ overpass on 28 September 1999 was also used; these data are useful since the sensor scans close to nadir. The solar channel DNs were also classified using the ISODATA algorithm (Fig. 1(d)).

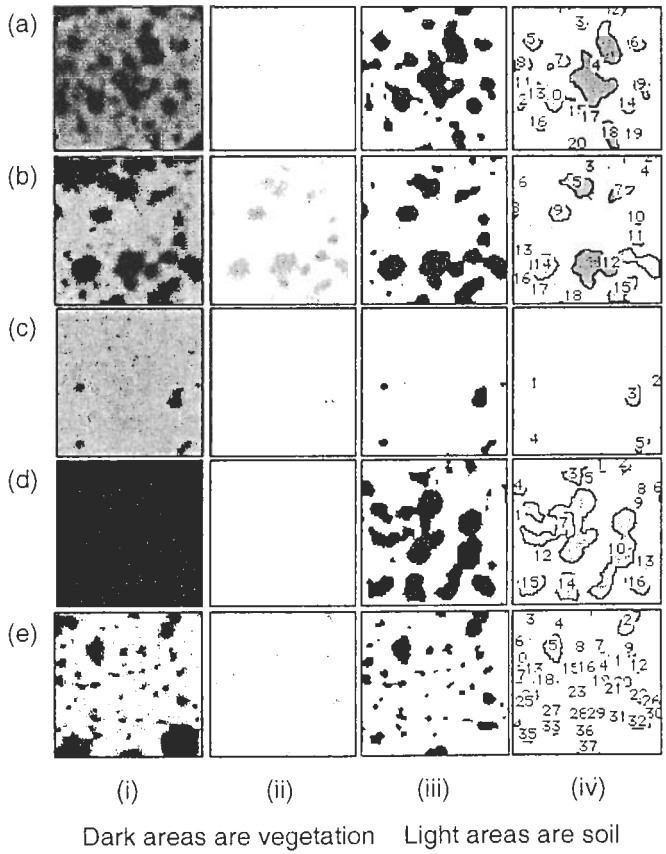

Fig. 2 Calculation of shrub density and cover from scanned aerial photography. Examples (a–e) are shown for four stages: (i) extracted sub-window, (ii) after background subtraction, (iii) after thresholding and (iv) outlined and labelled vegetation "particles".

RESULTS

MASTER reflectance data and associated geometries were extracted for each class. Figure 3 shows the 0.666 μm data plotted against view zenith angle for the eight classes derived from ETM+ data. In general there is a very consistent directional signal and only a small difference in the angular reflectance characteristics of the various cover types in this plane. The difference between back- and forward-scattering values is between 5 and 10% reflectance, necessitating corrections to these data prior to their use in validation studies; flying the aircraft so that angular impacts are at a minimum will not suffice. These results are also reflected in the data extracted from the classification

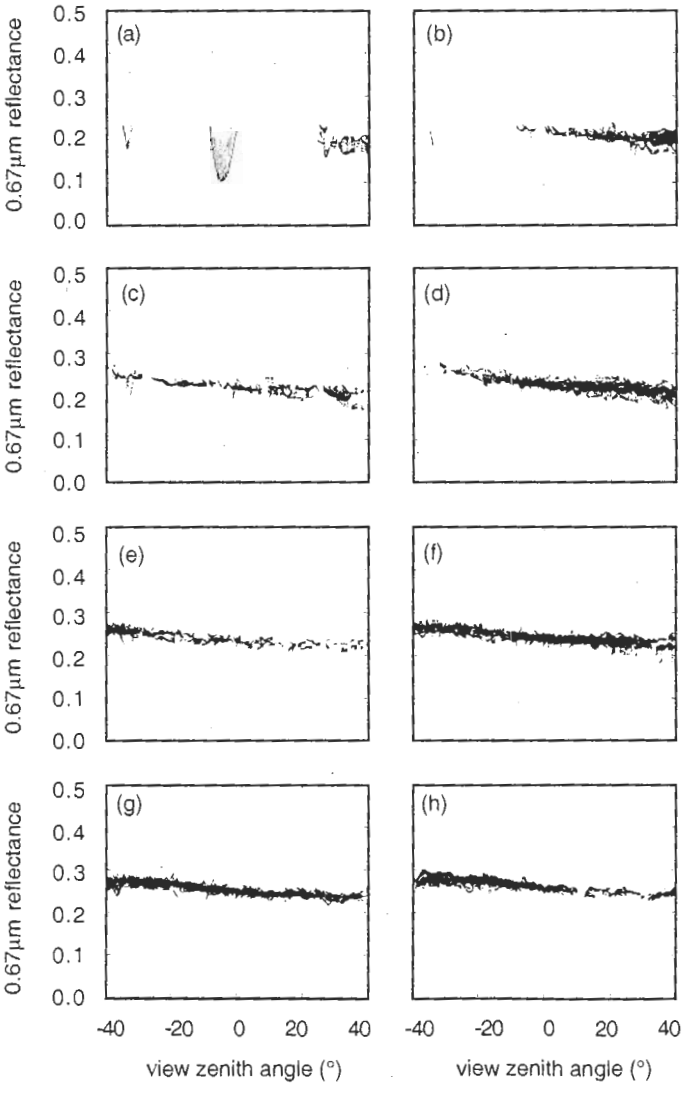

Fig. 3 Anisotropy in MASTER 0.67 μm reflectance data for eight ETM-derived classes.

of aerial photography. The MASTER data used here were acquired with relative azimuths of ~45° and ~135°; i.e. well away from the principal plane where the directional signal is strongest. The physical structure and composition of shrub-coppice dune landscapes are thus likely to have an important impact on reflectance anisotropy in MASTER solar wavelength data. The lack of variation in the angular signatures with cover type is likely due to the poor view/illumination geometry and the domination of the scene (up to 75% of areal cover) by very bright soils with lower reflectance anisotropy (Rango *et al.*, 2000). For small densely-vegetated patches such as mesquite and golden crownbeard (*V. encelioides*) communities, it is difficult to determine the directional signal (Fig. 3(a), which also indicates that the assumption of discrete cover types may be invalid). The accumulation of multi-angular signatures using data from a single MASTER overflight requires the selection of a scanning geometry closer to the principal plane, or use of other multidirectional data to adequately characterize the BRDF. Further research is required to determine whether a simple BRDF model might be adequate for angular corrections.

REFERENCES

Barnsley, M. J. (1994) Environmental monitoring using multiple-view-angle (MVA) remotely-sensed data. In: *Environmental Remote Sensing: From Regional to Global Scales* (ed. by G. Foody & P. Curran), 181–201. Wiley, Chichester, UK.

Chopping, M. J. (2000) Large-scale BRDF retrieval over New Mexico with a multiangular NOAA AVHRR data set. *Remote Sens. Environ.* **74**, 163–191.

DeSoyza, A. G., Whitford, W. G., Herrick, J. E., Van Zee, J. W. & Havstad, K. M. (1998) Early warning indicators of desertification: examples of tests in the Chihuahuan Desert. *J. Arid Environ.* **39**, 101–112.

Hlavka, C. A. (1986) Simulation of Landsat MSS spatial resolution with airborne scanner data. *NASA Technical Memorandum 86832*. NASA Center for Aerospace Research, USA.

Holben, B. N., Eck, T. F., Slutsker, I., Tanré, D., Buis, J. P., Setzer, A., Vermote, E., Reagan, J. A., Kaufman, Y. J., Makahjima, T., Lavenu, F., Jankowiak, I. & Smirnov, A. (1998) AERONET—A federated instrument network and data archive for aerosol characterization. *Remote Sens. Environ.* **66**, 1–16.

Kennedy, R. E., Cohen, W. B., & Takao, G. (1997) Empirical methods to compensate for a view-angle-dependent brightness gradient in AVIRIS imagery. *Remote Sens. Environ.* **62**, 277–291.

Kimes, D. S. (1983) Dynamics of directional reflectance factor distribution for vegetation canopies. *Appl. Optics* **22**(9), 1364–1372.

Leroy, M. & Bréon, F.-M. (1996) Angular signatures of surface reflectances from airborne POLDER data. *Remote Sens. Environ.* **57**, 97–107.

Privette, J. L. & Asner, G. P. (1999) The Prototype Validation Exercise (PROVE) for EOS land and atmosphere products. In: *Remote Sensing of the Earth—A Challenge for the 21st Century* (ed. by T. I. Stein) (Proc. 1999 Int. Geosci. & Remote Sens. Symp. (IGARSS), June–July 1999, Hamburg, Germany), 585–588. IEEE, Piscataway, New Jersey, USA.

Qi, J., Moran, M. S., Cabot, F. & Dedieu, G. (1995) Normalization of sun/view angle effects using spectral albedo-based vegetation indices. *Remote Sens. Environ.* **52**, 207–217.

Qi, J., Moran, M. S., Clarke, T. & Pinter, P. J. (1997) Practical techniques to correct bidirectional effects found in airborne remote sensing imagery. *Annual Research Report 1997*, US Water Conservation Lab., Phoenix, Arizona, USA.

Rango, A., Ritchie, J. C., Kustas, W. P., Schmugge, T. J. & Havstad, K. M. (1998) JORNEX: Remote sensing to quantify long-term vegetation change and hydrological fluxes in an arid rangeland environment. In: *Hydrology in a Changing Environment* (ed. by H. Wheater & C. Kirby), 585–590. John Wiley, London, UK.

Rango, A., Chopping, M., Ritchie, J., Havstad, K., Kustas, W. & Schmugge, T. (2000) Morphological characteristics of shrub-coppice dunes in desert grasslands of southern New Mexico derived from scanning LIDAR data. *Remote Sens. Environ.* **74**, 26–44.

Vermote, E., Tanre, D., Deuze, J. L., Herman, M. & Morcrette, J. J. (1997) Second Simulation of the satellite signal in the solar spectrum (6S): an overview. *IEEE Trans. Geosci. Remote Sens.* **35**(3), 675–686.